Radiofrequency field absorption by carbon nanotubes embedded in a conductive host

Mikhail V. Shuba,[1,a)] Gregory Ya. Slepyan,[2] Sergey A. Maksimenko,[2] and George W. Hanson[2,b)]
[1]*Institute for Nuclear Problems, Belarus State University, Bobruiskaya 11, 220030 Minsk, Belarus*
[2]*Department of Electrical Engineering, University of Wisconsin-Milwaukee, 3200 N. Cramer St., Milwaukee, Wisconsin 53211, USA*

(Received 11 August 2010; accepted 15 October 2010; published online 1 December 2010)

Understanding the electromagnetic response of carbon nanotubes (CNTs) in the radio frequency range is very important for experimental development of therapeutic and diagnostic CNT applications, including selective thermolysis of cancer cells and thermoacoustic imaging. In this study, we present the theory of electromagnetic wave scattering by several finite length CNT configurations, including singlewall CNT's having a surfactant coating, CNT bundles, and multiwall CNTs. Absorption cross-sections of these structures in a conductive host region are theoretically studied in the radio frequency range. Strong local field enhancement due to edge effects is predicted to be inherent to metallic singlewall CNTs in the near-field zone, providing an additional mechanism of energy dissipation in a conductive host. Due to the screening effect the application of singlewall CNTs for the enhancement of energy dissipation is more effective than the application of multiwall CNTs or CNT bundles at the same mass fraction of CNT inclusions. The presence of a lossy dielectric (surfactant) coating can significantly increase the absorption cross section of singlewall CNTs. © *2010 American Institute of Physics*. [doi:10.1063/1.3516480]

I. INTRODUCTION

Single-walled carbon nanotubes (SWCNT) are hexagonal networks of carbon atoms rolled up into a cylinder. Owing to their fascinating physical properties,[1] carbon nanotubes (CNTs) have aroused enormous interest in the scientific community due to wide applications ranging from chemical and biological sensors and actuators to field emitters to mechanical fillers for composite materials. In particular, carbon nanotubes are proposed as building blocks for the realization of different integrated circuits elements and electromagnetic devices, such as transmission lines,[2–5] interconnects,[6] nanoantennas,[7–10] and active elements—terahertz and infrared light emitters.[11–13]

Nowadays, due to the enhanced electromagnetic response of carbon nanotubes, they are considered as perspective nanoparticles for therapeutic applications including selective photothermolysis of cancer cells,[14–23] and photoacoustic and thermoacoustic imaging.[24,25] Note that plasmonic photothermal therapy using gold nanoparticles has emerged to be highly promising for cancer therapy and is fast developing.[26]

Applications of phototermolisis and photoacoustic imaging for medical purpose is limited by small (few centimeters) depth penetration of visible and infrared radiation in tissue. Thermoacoustic imaging refers to irradiating the sample with electromagnetic energy in the microwave and rf range and, in particular, provides deep tissue penetration and large sampling volumes. As theoretically shown in Ref. 27, SWCNTs can be considered as perspective thermal contrast agents at rf frequencies. The experimental studies of SWCNTs as thermal contrast agents at microwave frequencies are presented in Ref. 28. The first experiment on carbon nanotube-enhanced thermal destruction of cancer cells in a radiofrequency field[29] opens new possibilities for cancer treatment of deep tissues. Theoretical studies of CNT-enhanced microwave detection of breast cancer[30] and CNT-enhanced microwave discrimination of lesions[31] are also reported.

The conductivity of the components of a living cell vary in a wide range. As an example,[32] for liver cells the conductivity of cytoplasm is ≈ 0.5 S m^{-1} and the conductivity of nuclear and mitochondrial material is ≈ 5 S m^{-1}. Due to high media conductivity local energy dissipation enhancement can be realized by means of the CNTs local field enhancement. As shown in Ref. 33, due to edge effects, in the THz-range SWCNTs can enhance field intensity in a relatively large volume surrounding the nanotube (as much as 100 times larger than the volume occupied by the nanotube itself). This property, caused by the high aspect ratio and high conductivity of SWCNTs, also occurs at rf frequencies, and is not inherent to other known nanoparticles.

The aim of the present paper is to analyze the mechanism of electromagnetic energy dissipation provided by carbon nanotubes in a conductive host at radio frequencies. We present for the first time calculations of RF electromagnetic absorption cross sections of finite length electrically small (i) SWCNTs, (ii) bundles of SWCNTs, (iii) multiwall carbon nanotubes (MWCNT), and (iv) SWCNTs covered with a thin lossy dielectric. We shall show a strong dependence of absorption cross-section on the conductivity of the host media and demonstrate absorption enhancement provided by a lossy coating on SWCNTs.

a)Electronic mail: mikhail.shuba@gmail.com.
b)Electronic mail: george@uwm.edu.

 © 2010 American Institute of Physics

Downloaded 01 Dec 2010 to 129.89.58.128. Redistribution subject to AIP license or copyright; see http://jap.aip.org/about/rights_and_permissions

II. THEORY OF ELECTROMAGNETIC WAVE SCATTERING BY CNT IN RF RANGE

A. Scattering problem for coated SWCNT

Let a SWCNT with length L and radius R be coated by a dielectric layer having permittivity ε_s, internal radius R, and external radius $b>R$. In typical aqueous applications the dielectric coating will be a surfactant layer that inhibits nanotube agglomeration. The coated SWCNT is located in a host medium with permittivity ε_w. The origin of the chosen cylindrical coordinate system lies in the center of the SWCNT with axis z directed along the nanotube axis. The SWCNT will be considered as an infinitely thin hollow cylinder (with coordinate $-L/2<z<L/2$, $\rho=R$) located in a medium with permittivity

$$\varepsilon(\rho,z)=\begin{cases}\varepsilon_0, & \text{if} \quad \rho<R, & |z|<L/2\\ \varepsilon_s & \text{if} \quad b>\rho>R, & |z|<L/2\\ \varepsilon_w & \text{if} \quad \rho>b, & z\in[-\infty,+\infty]\\ \varepsilon_w & \text{if} \quad \rho<b, & |z|>L/2\end{cases}, \tag{1}$$

where $\varepsilon_0=8.85\times10^{-12}$ F/m. The incident field is polarized along the z axis $\mathbf{E}_{inc}(\mathbf{r},t)=\mathbf{E}_0\exp(i\omega t)$, where $\mathbf{E}_0=E_0(\mathbf{r})\mathbf{e}_z$ and ω is angular frequency. Ampère's law for electric and magnetic field vectors $\mathbf{E}$ and $\mathbf{H}$ in the whole space can be written as follows:

$$rot\mathbf{H}=i\omega\varepsilon\mathbf{E}+\mathbf{j}^{(c)}=i\omega\varepsilon_w\mathbf{E}+\mathbf{j}+\mathbf{j}^{(c)}, \tag{2}$$

where $\mathbf{j}^{(c)}$ is a current density induced on the SWCNT surface

$$\mathbf{j}^{(c)}=\sigma_c\delta(\rho-R)E_z\mathbf{e}_z, \tag{3}$$

and σ_c is the axial surface conductivity of the SWCNT; $\delta(\rho-R)$ is the Dirac delta function. In Eq. (2) we introduced an effective volume current density

$$\mathbf{j}=i\omega(\varepsilon-\varepsilon_w)\mathbf{E}=\sigma\mathbf{E}, \tag{4}$$

with an effective conductivity of the dielectric cylinder

$$\sigma=i\omega(\varepsilon-\varepsilon_w). \tag{5}$$

One can see that $\sigma=0$ and consequently $\mathbf{j}=0$ outside the cylindrical volume V, which occupies a space region $\rho<b$, $|z|<L/2$. The electromagnetic field satisfies the equation

$$\Delta\mathbf{E}+k^2\mathbf{E}=\frac{i\omega}{\varepsilon c^2}(\mathbf{j}+\mathbf{j}^{(c)}), \tag{6}$$

where $k=\omega\sqrt{\varepsilon_w\mu_0}$ is the wave number in the host region, $\mu_0=4\pi\times10^{-7}$ H/m, and c is the speed of light in vacuum. Assuming the SWCNT radius R and the external radius of the dielectric coating b to be small as compared to the wavelength in the host medium we neglect the azimuthal current on the SWCNT and in the coating. We also neglect azimuthal variations of current density $\mathbf{j}^{(c)}$ on the SWCNT and $\mathbf{j}$ in the coating; that is, we set $\mathbf{j}^{(c)}(z,\rho)=j^{(c)}(z)\delta(\rho-R)\mathbf{e}_z$ and $\mathbf{j}=j_z(z,\rho)\mathbf{e}_z+j_\rho(z,\rho)\mathbf{e}_\rho$. As a result, the scattered fields are azimuthally symmetric. We shall consider a coating with conductivity much smaller than the conductivity of the SWCNT, that is

$$\omega\left|\int_0^b(\varepsilon-\varepsilon_w)\rho d\rho\right|\ll R|\sigma_c|. \tag{7}$$

As the axial component of the scattered field is continuous and consequently approximately the same throughout the small volume V, then, according to Eqs. (3) and (4) and condition (7) the inequality $\int_0^b j_z\rho d\rho\ll j^{(c)}R$ holds. Then, in Eq. (6) together with $\mathbf{j}^{(c)}$ we take into account only the radial component of the current in the coating, that is, we set $\mathbf{j}=j_\rho(z,\rho)\mathbf{e}_\rho$.

The solution of Eq. (6) has the form

$$\mathbf{E}=\mathbf{E}_0+\mathbf{E}^{(c)}+\mathbf{E}^{(d)}, \tag{8}$$

where

$$\mathbf{E}^{(c)}=\frac{R}{i\omega\varepsilon_w}(\text{grad div}+k^2)\int_{-L/2}^{L/2}j^{(c)}(z')\mathbf{e}_z\times\int_0^{2\pi}g(z-z',R,\rho,\phi)d\phi dz', \tag{9}$$

is the scattered field induced by the surface current on the SWCNT, and

$$\mathbf{E}^{(d)}\cong\frac{1}{i\omega\varepsilon_w}(\text{grad div}+k^2)\int_V\mathbf{e}_{\rho'}j_{\rho'}(\mathbf{r}')g(|\mathbf{r}-\mathbf{r}'|)d^3\mathbf{r}', \tag{10}$$

is the scattered field induced by the radial current in the dielectric coating, and

$$g(|\mathbf{r}-\mathbf{r}'|)=g(z-z',\rho,\rho',\phi)=\exp[-ik|\mathbf{r}-\mathbf{r}'|]/[4\pi|\mathbf{r}-\mathbf{r}'|], \tag{11}$$

$$|\mathbf{r}-\mathbf{r}'|=\sqrt{(z-z')^2+\rho^2+\rho'^2-2\rho\rho'\cos(\phi)}. \tag{12}$$

The electric field vectors $\mathbf{E}^{(d)}$ and $\mathbf{E}^{(c)}$ in Eqs. (9) and (10) are taken in the form to satisfy the radiation condition.[34] As shown in the Appendix, the component $E_z^{(d)}$ is much smaller than $E_z^{(c)}$ and can be further omitted. The other components $E_z^{(c)}$, $E_\rho^{(c)}$, and $E_\rho^{(d)}$ inside the dielectric coating are calculated in the Appendix and presented by Eqs. (A1), (A6), and (A11), respectively.

Substituting Eq. (8) into Eqs. (3) and (4) and taking into account Eqs. (A1), (A6), and (A11) we arrive at the system of equations

$$j^{(c)}(z)=E_0\sigma_c+\frac{R\sigma_c}{i\omega\varepsilon_w}\int_{-L/2}^{L/2}j^{(c)}(z')\times\int_0^{2\pi}\left(\frac{\partial^2}{\partial z^2}+k^2\right)g(z-z',R,R,\phi)d\phi dz', \tag{13}$$

$$j_\rho(\rho,z)\cong-\frac{R\sigma}{i\omega\varepsilon_s\rho}\frac{\partial j^{(c)}}{\partial z}. \tag{14}$$

Equation (13) is an integral equation for surface current density $j^{(c)}$ on the SWCNT surface. The electric field E_0 in Eq. (13) can be considered to be z-independent if the condition $\omega L|\sqrt{\varepsilon_w}|/(2\pi c)\ll1$ holds. This condition is satisfied at

Downloaded 01 Dec 2010 to 129.89.58.128. Redistribution subject to AIP license or copyright; see http://jap.aip.org/about/rights_and_permissions

all values ω, ε_w, and L applied below in our considerations. To solve the Eq. (13) the integral on the right side of Eq. (13) is numerically handled by a quadrature formula, thereby transforming Eq. (13) into a matrix equation. Solution of matrix equation gives axial current density along SWCNT. After the solution of Eq. (13) and substitution $j^{(c)}$ into Eq. (14) the component j_ρ in the dielectric layer can be easily found. Then the scattered field and total field can be calculated from expressions (9), (10), and (8), respectively.

B. Integral equations for scattering problem of SWCNT-bundle

The integral Eq. (13) does not depend on the coating dielectric parameters and holds true for an uncoated SWCNT. This equation can be generalized in the case of the scattering problem for a bundle containing N parallel SWCNTs of length L. At frequencies far away from interband resonances azimuthally nonsymmetric electric current densities are not excited in SWCNTs because the relevant conductivities vanish. Then, restricting ourselves to azimuthally symmetric electric current densities in the SWCNTs forming the bundle and applying the many-body technique we arrive at a system of integral equations[35]

$$j_m^{(c)}(z) = E^{(0)}(z)\sigma_m^{(c)} + \frac{\sigma_m^{(c)}}{i\omega\varepsilon_w}\sum_{l=1}^{N} R_l \int_{-L/2}^{L/2} j_l^{(c)}(z') \times \int_0^{2\pi} \left(\frac{\partial^2}{\partial z^2} + k^2\right) g(z-z', R_m, d_{ml}, \phi) d\phi dz'. \quad (15)$$

This is a system of N integral equations for surface current density $j_m^{(c)}$ $(m,l \in [1,N])$ on the surface of the m-th SWCNT with radius R_m and conductivity $\sigma_m^{(c)}$; d_{ml} $(l \neq m)$ is the distance between the axes of the l-th and m-th SWCNTs; $d_{mm} = R_m$. As SWCNT-bundle cross section is much smaller than the wavelength of the incident electromagnetic wave, then the external field $E^{(0)}$ in Eq. (15) is considered to be identical for all tubes forming the bundle.

C. Integral equations for scattering problem of MWCNT

Let us consider a MWCNT consisting of N shells; the m-th shell $(m \in [1,N])$ of the MWCNT has radius R_m and conductivity $\sigma_m^{(c)}$. We shall suppose that adjacent shells are incommensurate[36] and neglect electron tunneling between shells. The conductivity of the m-th shell is considered to be the same as the conductivity of a SWCNT with the same geometrical parameters. The scattering problem for MWCNTs from terahertz to visible frequencies is presented in detail in Ref. 36. However, the technique presented in[36] is based on Hallén-type integral equations. In solving numerically the Hallén-type integral equations by the collocation method we arrive at an $\tilde{N} \times \tilde{N}$ matrix, where two columns contain elements $\exp(ikz_j)$, $z_j = -L/2 + L(j-1)/(\tilde{N}-1)$, $j = 1,2 \ldots \tilde{N}$. This matrix is close to degenerate when $|k|L \ll 1$, which leads to instability of the numerical matrix inversion in the quasistatic regime. At realistic parameters for the MWCNT the quasistatic regime occurs in the rf-range. Therefore, to solve the scattering problem for MWCNTs in the rf-range we do not apply Hallén-type equations, but directly solve the system of integral equations in the form

$$j_m^{(c)}(z) = E^{(0)}(z)\sigma_m^{(c)} + \frac{\sigma_m^{(c)}}{i\omega\varepsilon_w}\sum_{l=1}^{N} R_l \int_{-L/2}^{L/2} j_l^{(c)}(z') \times \int_0^{2\pi} \left(\frac{\partial^2}{\partial z^2} + k^2\right) g(z-z', R_m, R_l, \phi) d\phi dz', \quad (16)$$

This is a system of integral equations for the current $j_m^{(c)}$ $(m \in [1,N])$ on the surface of the m-th shell of the MWCNT. Numerical solution of this system is stable and shall be applied below for numerical calculation of the energy dissipation in MWCNT.

D. SWCNT absorption parameters

For a single coated SWCNT, the power dissipated in the SWCNT coating P_s and in the SWCNT itself P_c can be calculated as

$$P_s = \pi\omega \,\mathrm{Im}[\varepsilon_s] \int_R^b \int_{-L/2}^{L/2} [|E_z|^2 + |E_\rho|^2] \rho dz d\rho, \quad (17)$$

$$P_c = \pi R \,\mathrm{Re}\left(\frac{1}{\sigma_c}\right) \int_{-L/2}^{L/2} |j^{(c)}|^2 dz. \quad (18)$$

The intensity of the scattered field near a SWCNT can be much higher than the intensity of the incident field. If the host is a lossy medium, than large intensity of the scattered field leads to large absorption in the host. In order to calculate dissipation of the scattered field in the host we introduce a cylindrical cell with radius $R_{\mathrm{cell}} \gg R$ and length equal to the nanotube length L; the cell volume is $V_{\mathrm{cell}} = \pi R_{\mathrm{cell}}^2 L$. The SWCNT is located inside this cell on the cell axis. Then, the power dissipated in the host medium of the cell is

$$P_w = \pi\omega \,\mathrm{Im}[\varepsilon_w] \int_b^{R_{\mathrm{cell}}} \int_{-L/2}^{L/2} [|E_z|^2 + |E_\rho|^2] \rho dz d\rho, \quad (19)$$

and the power dissipated in the cell without a SWCNT, exposed only to the external field, is

$$P_{0w} = \pi\omega \,\mathrm{Im}[\varepsilon_w] \int_0^{R_{\mathrm{cell}}} \int_{-L/2}^{L/2} |E_0|^2 \rho dz d\rho \quad (20)$$

Let us introduce an absorption cross section Λ_0 and a normalized absorption cross section Λ of a SWCNT in a lossy surrounding,

$$\Lambda_0 = \frac{P_w - P_{0w} + P_c + P_s}{I_0}, \quad (21)$$

$$\Lambda = \Lambda_0 / S, \quad (22)$$

where $I_0 = 0.5|\sqrt{\varepsilon_w/\mu_0}||E_0|^2\cos(\varphi)$ is the intensity of the incident field, $\varphi = \arg[\sqrt{\varepsilon_w}]$, and $S = 2\pi RL$ is the area of the SWCNT surface. For sufficiently large R_{cell} the value of Λ is approximately independent of cell volume.

Downloaded 01 Dec 2010 to 129.89.58.128. Redistribution subject to AIP license or copyright; see http://jap.aip.org/about/rights_and_permissions

For a suspension of carbon nanotubes we introduce a new parameter θ—the relative absorption rate—characterizing the relation between energy dissipation in a SWCNT-suspension and energy dissipation in a pure suspension without SWCNTs,

$$\theta = \frac{P_w + P_c + P_s}{P_{0w}}. \tag{23}$$

For calculation of the values P_w, P_{0w} included in Eq. (23), the cell volume V_{cell} should be taken from the concentration n of SWCNTs in suspension: $V_{\text{cell}}=1/n$. The value θ makes sense for diluted SWCNT suspensions, where electromagnetic interactions between SWCNTs can be neglected and, consequently, the energy dissipation in the suspension is proportional to the SWCNT concentration. The small electromagnetic interactions between metallic SWCNTs is provided at small CNT volume fraction $f<0.001$ of non-agglomerated metallic SWCNTs suspension. Note that f denotes the volume fraction occupied by the SWCNTs (conceived as cylinders of volume $\pi R^2 L$). Small electromagnetic interactions between semiconducting SWCNTs permits the application of parameters θ at higher values of volume fraction $f<0.1$. In such an approximation, assuming the heat convection and heat radiation from the suspension to be small, the value θ can be expressed through the relative heating rate of the suspension

$$\theta = \frac{\partial T_2/\partial t}{\partial T_1/\partial t}, \tag{24}$$

where $\partial T_2/\partial t \propto P_w + P_c + P_s$ is the heating rate of the SWCNTs suspension and $\partial T_1/\partial t \propto P_{0w}$ is the heating rate of the pure liquid without SWCNTs.

Let us note that θ can be obtained from measurement of the SWCNT suspension heating rate.

Formulas (21)–(23) can also be applied for uncoated CNTs (SWCNTs, MWCNTs, SWCNT bundles). In these cases $P_s=0$, P_c is the power dissipated by the CNT, and S is a sum of surface areas of all graphene shells of the CNT.

III. NUMERICAL RESULTS

In all calculations the conductivity of metallic SWCNTs was taken using the Drude-law[2] with relaxation time 2×10^{-14} s (relaxation due to optical phonons[38]). The influence of other mechanisms (impurities, defects, doping, and the influence of surrounding media) on electron inelastic scattering are less than the influence of optical phonons, and consequently cannot change strongly the chosen small relaxation time. As demonstrated in Ref. 37 the electron relaxation time at terahertz frequencies equals 3.3×10^{-14} s at room temperature, which is close to the chosen value. As discussed below, the absorption parameters of metallic SWCNTs in a conductive host does not change substantially with increasing τ from 2×10^{-14} s to larger magnitudes.

Existing experiments at high (terahertz) frequencies[38] and dc[39] show that the conductivity of semiconducting SWCNTs is only several orders of magnitude lower than the conductivity of metallic SWCNTs, rather than the many orders of magnitude expected from Drude theory. This can be explained by impurities and atmospheric oxygen doping in SWCNTs. Therefore, for calculations we shall suppose the conductivity of semiconducting SWCNTs to be 1000 times lower than the conductivity of metallic SWCNTs with the same radius. For example, the axial surface conductivity of metallic (15,0) and semiconducting (16,0) zigzag SWCNTs were taken respectively as (i) $1.46\times10^{-3}+i1.84\times10^{-9}$ S and $1.37\times10^{-6}+i1.72\times10^{-12}$ S, at frequency 10 MHz and (ii) $1.46\times10^{-3}+i1.84\times10^{-8}$ S and $1.37\times10^{-6}+i1.72\times10^{-11}$ S at frequency 100 MHz

We shall demonstrate our numerical results in the radio frequency range from 10 up to 200 MHz. In all calculations the dispersion law for the host permittivity is

$$\varepsilon_w = 80\varepsilon_0 - \frac{i\sigma_w}{\omega}, \tag{25}$$

where σ_w is the host medium conductivity; the numerical coefficient 80 is a relative dielectric constant, which is taken to be the same as for water. The relative dielectric constant of water varies slightly (by several percent) in the considered frequency range, although we will neglect this variation in our calculations. The last formula is applied for cytoplasm and nuclear media of living cells.[32] We shall suppose σ_w =const inside the chosen frequency range.

The conductivity of the components of a living cell vary in a wide range. Therefore, we shall analyze the energy dissipation caused by CNTs for different host conductivity σ_w. For numerical calculations of relative absorption rate θ of the SWCNTs suspension we shall take the SWCNT concentration n and radius of the cylindrical cell R_{cell} corresponding to a SWCNT mass fraction of 50 mg/L, which is considered to be nontoxic for living cells.[40] Let us repeatedly note that in the case of dilute SWCNT suspensions the relation $\theta \propto n$ is true.

A. Near field enhancement in SWCNT

Figure 1 shows the space distribution of intensity enhancement factor $\xi=|E|^2/|E_0|^2$ near the right half of a metallic [Fig. 1(a)] and semiconducting [Fig. 1(b)] SWCNT. Near the left half of the tube the distribution of ξ is the same.

Due to edge effects a large surface density of electric charge concentrates near the SWCNT edges. This charge induces an electric field with large radial component, resulting in strong field intensity enhancement outside the SWCNT. The effect of charge separation in SWCNTs has an electrostatic character, i.e., the metallic SWCNT polarization and near-field enhancement does not depend on the SWCNT conductivity, and, consequently, does not depend on electron relaxation time $\tau>2\times10^{-14}$ s.

Thus, SWCNTs concentrate electromagnetic energy near the SWCNT surface, and therefore enhance power absorption in the conductive host. Let us note that semiconducting tubes can concentrate electromagnetic energy only at low host conductivity $\sigma_w<0.5$ S m^{-1} and at low frequency (below 100 MHz). Either at higher host conductivity σ_w or at higher frequency the depolarization effect in semiconducting SWCNTs diminishes, and scattered field intensity near the SWCNT surface becomes comparable with the intensity of

Downloaded 01 Dec 2010 to 129.89.58.128. Redistribution subject to AIP license or copyright; see http://jap.aip.org/about/rights_and_permissions

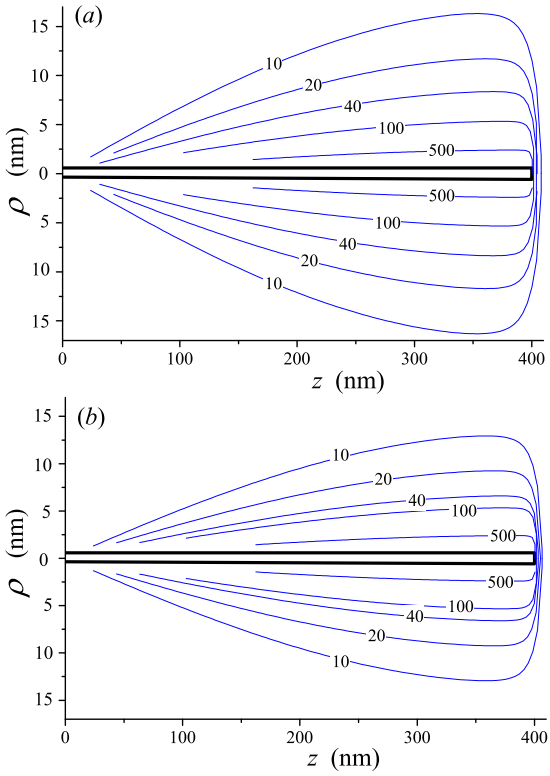

FIG. 1. (Color online) The constant-value lines of the intensity enhancement factor $\xi(r)$ in the vicinity of the right half of uncoated (a) metallic (15,0) and (b) semiconducting (16,0) zigzag SWCNTs with length $L=0.8$ μm. The right half of the SWCNT is shown by the thick line. The relative dielectric constant of the host is $\varepsilon_w/\varepsilon_0=80-18i$ ($\sigma_w=0.01$ S/m). The frequency is $\omega/2\pi=10$ MHz.

the incident field. Further, the axial component of the scattered electric field near the SWCNT surface is approximately equal to and oppositely directed to the axial component of the incident field. As a result, the axial component of the resulting field near the SWCNT surface is much smaller than the axial component of the incident field.

B. Absorption by SWCNTs in a conductive host

Figure 2 shows the normalized absorption cross section Λ for semiconducting and metallic SWCNTs versus the host conductivity σ_w at different frequencies. At small host conductivity $\sigma_w<0.1$ S m^{-1} the absorption cross section Λ for semiconducting SWCNTs exceeds the value Λ for metallic

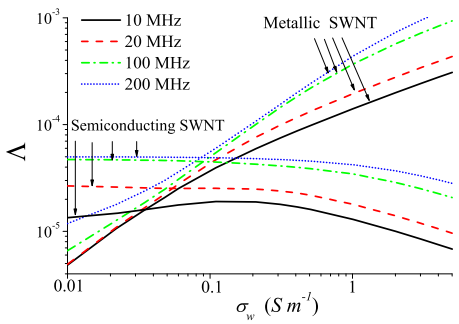

FIG. 2. (Color online) Normalized absorption cross section Λ for uncoated semiconducting (16,0) and metallic (15,0) SWCNT vs the conductivity σ_w of surrounding media at different frequencies.

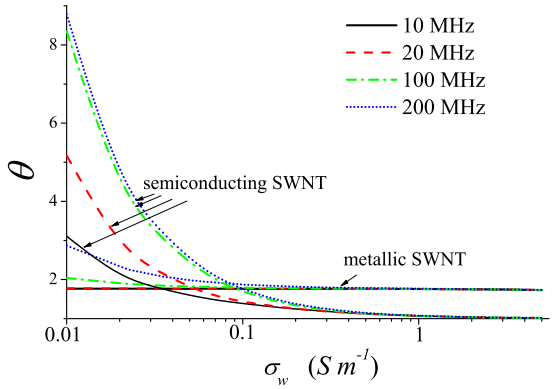

FIG. 3. (Color online) Relative absorption rate θ for uncoated semiconducting (16,0) and metallic (15,0) SWCNT vs the conductivity σ_w of surrounding media at different frequencies. $L=0.8$ μm. Mass fraction of SWCNT is 50 mg/L.

SWCNTs, while at larger conductivity the value Λ for metallic tubes exceeds Λ for semiconducting tubes. This different behavior is explained by the different dominant mechanisms of energy dissipation: for metallic tubes the energy is dissipated mostly by the host i.e., $P_w-P_{0w}\gg P_c$, whereas for semiconducting tubes the energy is dissipated mostly by the tube i.e., $P_c\gg P_w-P_{0w}$.

The power P_c dissipated in a SWCNT increases with increasing frequency, while the value P_w-P_{0w} varies only slightly in the considered frequency range (from 10 up to 200 MHz). Therefore, the absorption cross section Λ of both semiconducting and metallic SWCNTs increases with increasing frequency (see Fig. 2).

Figure 3 shows the relative absorption rate θ for semiconducting SWCNT and metallic SWCNT suspensions versus the conductivity σ_w of surrounding media at different frequencies. The SWCNT suspensions have volume fraction $f=1.9\times10^{-5}$, corresponding to 50 mg/L mass fraction of (15,0) SWCNTs.

As demonstrated in Fig. 3, the rate of energy dissipation in the suspension with semiconducting SWCNTs at 200 MHz and $\sigma_w=0.01$ S m^{-1} is about eight times larger than for liquid without SWCNTs and about three times larger than for suspensions with metallic SWCNTs. Thus at small values of surrounding conductivity σ_w the energy dissipation is stronger for suspensions with semiconducting SWCNTs than for suspensions with metallic SWCNTs. The same tendency was illustrated in Ref. 27 for the case of a non-absorbing host.

An increase in the host conductivity σ_w leads to an increase in the dissipated power in a host without CNTs P_{0w}, while the power P_c dissipated in semiconducting SWCNTs varies only slightly with host conductivity variation. As a result, the relative absorption rate θ for semiconducting SWCNTs decreases with host increasing conductivity σ_w, while the value θ for suspensions with metallic SWCNTs remains constant with σ_w increasing (see Fig. 3). Thus at high values of the host conductivity the application of metallic SWCNTs for absorption enhancement is more preferable than application of semiconducting SWCNTs. Calculations show that the values of Λ and θ presented in Figs. 2

Downloaded 01 Dec 2010 to 129.89.58.128. Redistribution subject to AIP license or copyright; see http://jap.aip.org/about/rights_and_permissions

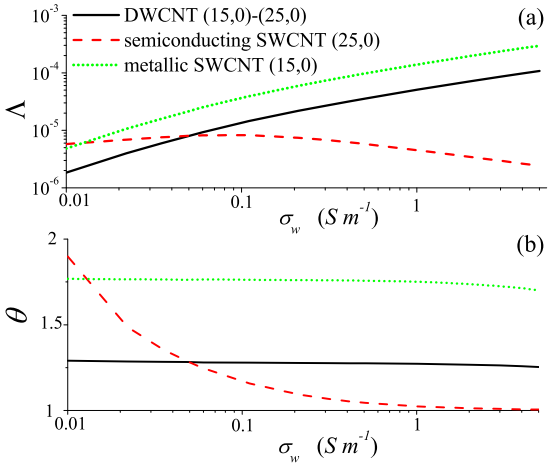

FIG. 4. (Color online) (a) Normalized absorption cross section Λ and (b) relative absorption rate θ for uncoated semiconducting (25,0) and metallic (15,0) SWCNTs and DWCNT (15,0)–(25,0) vs the conductivity σ_w of surrounding media. The frequency is 10 MHz, L=0.8 μm, and the CNTs mass fraction is 50 mg/L.

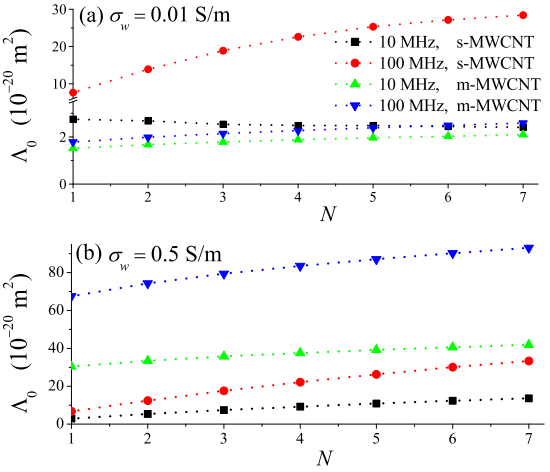

FIG. 5. (Color online) Dependencies of absorption cross section Λ_0 on the number of shells N for uncoated MWCNTs containing only metallic shells (m-MWCNT) and only semiconducting shells (s-MWCNT) at different frequencies (10 and 100 MHz) and different host conductivities [(a) σ_w =0.01 S/m and (b) σ_w=0.5 S/m]. L=0.8 μm. The lth shell of m-MWCNT and s-MWCNT has a (15+9l,0) and (16+9l,0) zigzag configuration, respectively, $l \in [1,N]$.

and 3 for metallic CNTs do not change with increasing the electron relaxation time from the chosen value of 2×10^{-14} s.

C. Absorption of MWCNTs in a conductive host

Calculations carried out for MWCNTs of length up to 10 μm show that due to edge effects the outmost metallic shell strongly diminishes the incident field inside the structure (i.e., the outmost metallic shell in MWCNTs screens the internal shells). Calculations shows that the main contribution to energy dissipation in MWCNTs is from the outmost metallic shell. Therefore, dissipated power $P_w+P_s-P_{0w}$ associated with MWCNTs approximately equals that of the outmost metallic shell. As a result, the normalized absorption cross section Λ of MWCNTs is less than Λ for metallic SWCNTs.

We also found that the outmost metallic shell in MWCNTs screens the semiconducting layers with larger diameters. To illustrate this effect we present in Fig. 4 the dependences $\Lambda(\sigma_w)$ and $\theta(\sigma_w)$ for a double wall CNT (DWCNT) (15,0)–(25,0) with internal metallic shell (15,0) and external semiconducting shell (25,0).

Figure 4 also shows the dependencies $\Lambda(\sigma_w)$ and $\theta(\sigma_w)$ for semiconducting (25,0) and metallic (15,0) SWCNTs. As shown in Fig. 4, the dependencies $\Lambda(\sigma_w)$ and $\theta(\sigma_w)$ for DWCNT and metallic SWCNT have identical behavior. However the metallic SWCNT has values of $\Lambda(\sigma_w)$ and $\theta(\sigma_w)$ which are about two times larger than for the DWCNTs. The reason is that the axial component of the resulting field near the metallic shell is strongly diminished by the depolarizing field, in comparison with the axial component of the incident field. As a result, the power dissipated in the semiconducting shell (25,0) of the DWCNT is much less than the power dissipated in a single semiconducting SWCNT (25,0). Thus, due to the very high aspect ratio of SWCNTs the screening effect results not only in axial field diminishment inside metallic shells but also in the diminishing of the axial field component outside the metallic shell.

Figure 5 shows the dependencies of absorption cross section Λ_0 on the number of shells N for two extreme cases: (i) for MWCNTs containing only metallic shells (m-MWCNT) and (ii) for MWCNTs containing only semiconducting shells (s-MWCNT). As shown in Fig. 5, due to screening effects in m-MWCNTs the value Λ_0 slightly increases with N increasing. The screening effect in s-MWCNT at low host conductivity (σ_w=0.01 S/m) and low frequency (10 MHz) even results in Λ_0 decreasing with N increasing. Since at high frequency or high host conductivity the screening effect is small in s-MWCNTs, the value Λ_0 for these tubes increases about three times with increasing N from 1 to 7.

Let us also note that the maximal value of Λ_0 corresponds (i) to s-MWCNTs at low host conductivity (σ_w =0.01 S/m) and high frequency (100 MHz), when screening effects are small and energy effectively dissipates in all shells of s-MWCNTs [see Fig. 5(a)] and (ii) to m-MWCNTs at high host conductivity (σ_w=0.5 S/m) [see Fig. 5(b)], when dissipation in host media is large due to strong field enhancement by m-MWCNTs.

Calculations show that due to screening effects the absorption cross-section Λ_0 of MWCNTs containing both metallic and semiconducting shells is approximately the same as Λ_0 for m-MWCNTs. Thus, the screening effect strongly diminishes the energy dissipation in MWCNT shells. As a result, the application of SWCNTs for absorption enhancement is more preferable than application of MWCNTs with the same mass fraction of CNT inclusions.

D. Absorption of SWCNTs bundle in the conductive host

Figure 6 illustrates the normalized absorption cross section Λ of a SWCNT bundle in the host with conductivity σ_w=0.5 S m^{-1} (a), and σ_w=0.01 S m^{-1} (b) versus the number of tubes in the bundle. Due to the field screening effect

Downloaded 01 Dec 2010 to 129.89.58.128. Redistribution subject to AIP license or copyright; see http://jap.aip.org/about/rights_and_permissions

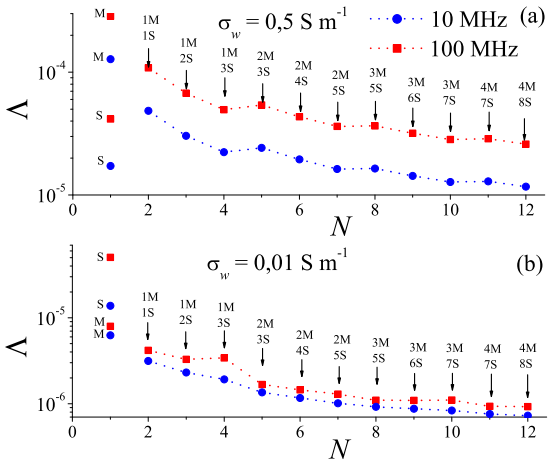

FIG. 6. (Color online) Normalized absorption cross section Λ of an uncoated bundle of SWCNTs in liquid with conductivity σ_w=0.5 S m^{-1} (a), and σ_w=0.01 S m^{-1} (b) vs the number of tubes in the bundle, N. The bundles consist of semiconducting (16,0) and metallic (12,0) SWCNTs. The letters "S" and "M" mean Λ for the single semiconducting and metallic SWCNTs, respectively. The abbreviation, for example, 2M-4S means that the bundle consist of two metallic and four semiconducting SWCNTs. L =0.8 μm.

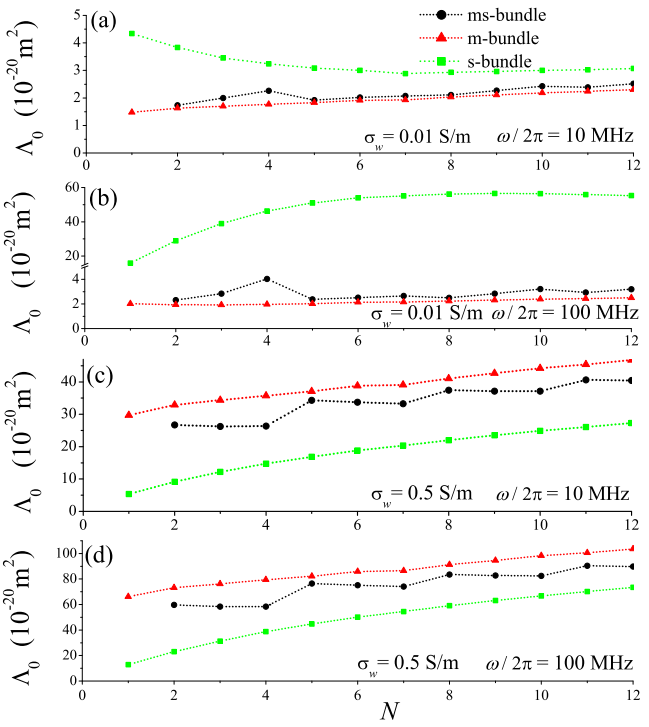

FIG. 7. (Color online) Absorption cross section Λ_0 for uncoated SWCNT bundles vs the number N of tubes in bundle at σ_w=0.01 S/m, $\omega/2\pi$ =10 MHz (a); σ_w=0.01 S/m, $\omega/2\pi$=100 MHz (b); σ_w=0.5 S/m, $\omega/2\pi$ =10 MHz (c); and σ_w=0.5 S/m, $\omega/2\pi$=100 MHz (d). The graphics depicted by black circles corresponds to bundle described in Fig. 6, that is the bundle of mixed semiconducting and metallic SWCNTs. Triangles and boxes corresponds to the bundles containing of only metallic (16,0) SWCNTs (m-bundle) and only semiconducting (12,0) SWCNTs (s-bundle), respectively. L=0.8 μm.

(discussed in the previous section) the dissipated power in the semiconducting tubes included into the bundle is strongly diminished compared with the dissipated power in single semiconducting tubes. Therefore, as Fig. 6 demonstrates, the value Λ decreases with the increasing of the number of tubes in the bundle. Note that this is partly due to the total surface area S increasing with bundle size.

Let us consider the absorption cross section Λ_0 of SWCNT bundles in liquids with different conductivities. Figure 7 shows the dependence of Λ_0 on the number N of SWCNTs in bundles (i) containing only metallic tubes (m-bundle) (ii) containing only semiconducting tubes (s-bundle) and (iii) containing a mixture of metallic and semiconducting SWCNTs (ms-bundle). At small host conductivity σ_w =0.01 S m^{-1} the value Λ_0 of the ms-bundle (i) increases with the addition of the semiconducting tubes and (ii) decreases with the addition of the metallic tubes [see Figs. 7(a) and 7(b)]. At larger host conductivity σ_w=0.5 S m^{-1} the main contribution to energy dissipation is given by the metallic tubes of the bundle, whereas the contribution of semiconducting SWCNTs is negligibly small [see Figs. 7(c) and 7(d)].

Let also note that the screening effect is pronounced for s-bundles at smaller frequencies and small host conductivities. Due to a significant screening effect at 10 MHz the value of Λ_0 for s-bundles decreases with N increasing [Fig. 7(a)]. At the higher frequency of 100 MHz the screening effect for s-bundles with N not large is smaller, resulting in the value of Λ_0 increasing with N increasing [see Fig. 7(b)].

A comparison of absorption cross section of a single metallic SWCNT and of a ms-bundle containing 12 SWCNTs (see Fig. 7) shows that energy dissipation in the bundle is comparable with energy dissipation in a metallic SWCNT. Figure 7 demonstrates that at small host conductivity the s-bundles are preferable to realize maximal absorption enhancement, whereas at high host conductivity the m-bundles are the best candidates for realization of maximal absorption enhancement.

Thus for increasing energy dissipation in the radio frequency range the application of SWCNTs is more preferable than the application of MWCNTs or bundles of SWCNTs with the same mass fraction of CNT inclusions. However, for a fixed number density of inclusions, from Figs. 5 and 7 it can be seen that in some cases MWCNTs or CNT bundles may be preferable to SWCNTs for increasing absorption.

E. Absorption of coated CNT in conductive host

Due to strong field enhancement near the surface of carbon nanotubes the presence of a lossy coating on a SWCNT can increase the value of absorption cross section Λ and heating rate. Since CNTs in aqueous environments are commonly coated with surfactants to prevent clumping, the presence of a surfactant coating is an important aspect to consider. The enhancement in power absorbed can be achieved by two ways; (i) If $\mathrm{Im}[\varepsilon_s] > \mathrm{Im}[\varepsilon_w]$ the absorption enhancement occurs due to the greater absorption in the coating than would have occurred in the host. (ii) If $|\varepsilon_w| > |\varepsilon_s|$, then according to Eqs. (A6) and (A12) the radial field component in the coating exceeds by approximately $|\varepsilon_w/\varepsilon_s|$ times that of the radial field component in the host. As a result, power

Downloaded 01 Dec 2010 to 129.89.58.128. Redistribution subject to AIP license or copyright; see http://jap.aip.org/about/rights_and_permissions

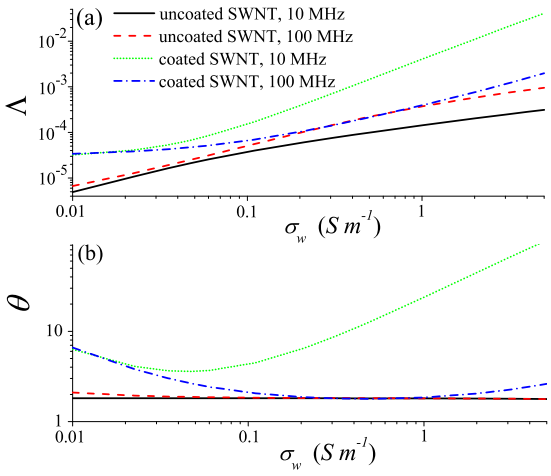

FIG. 8. (Color online) Normalized absorption cross section Λ of coated and uncoated (15,0) metallic SWCNTs vs the host conductivity at different frequencies. (b) Relative absorption rate θ for suspension of coated and uncoated (15,0) metallic SWCNTs. The relative dielectric constant of coating is $\varepsilon_s/\varepsilon_0=4-0.9i$ and $\varepsilon_s/\varepsilon_0=4-0.09i$ at 10 MHz and 100 MHz, respectively. The external radius of the coating is 3.4 nm. SWCNT mass fraction is 50 mg/L.

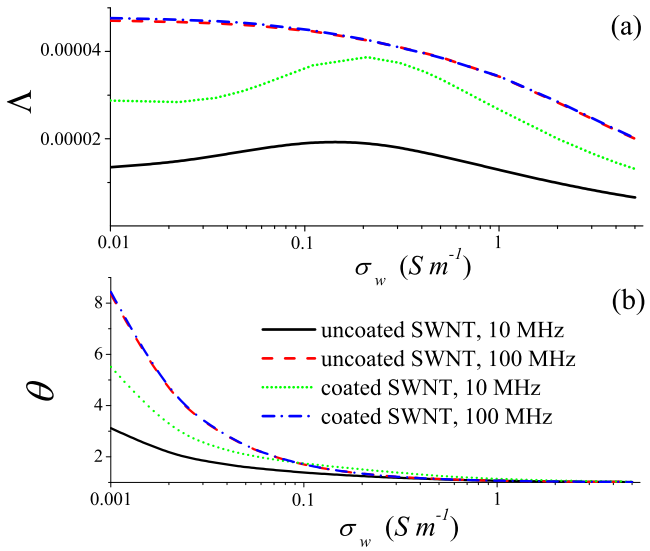

FIG. 9. (Color online) The same as in Fig. 8 but for semiconducting (16,0) SWCNTs.

dissipation in the coating is higher than in the host with an identical volume, even at the condition $\mathrm{Im}[\varepsilon_w]\approx\mathrm{Im}[\varepsilon_s]$.

As very little seems to be known about dielectric properties of CNT surfactants in the megahertz frequency range, for illustration purposes in our numerical calculations we assigned ε_s to have a reasonable value that is likely to be in the range of realistic surfactant materials.

Figure 8 shows the normalized absorption cross section Λ of coated and uncoated (15,0) metallic SWCNTs versus the conductivity of the surrounding medium at different frequencies. One can see from Fig. 8 that at 10 MHz the coating leads to Λ increasing 10–100 times, depending on the conductivity of the surrounding host medium. For small host conductivity at 100 MHz, due to the coating the value of Λ increases by 1.5–10 times as compared with the value of Λ for an uncoated SWCNT. Enhancement of Λ strongly depends on the ratio $|\varepsilon_w/\varepsilon_s|$. In order to obtain the largest value of Λ we should take the lossy coating with the largest possible ratio $|\varepsilon_w/\varepsilon_s|$.

Figure 9 shows the normalized absorption cross section Λ of coated and uncoated semiconducting SWCNTs versus the conductivity of the surrounding medium at different frequencies. As shown in Fig. 9, the coating practically does not change the value of Λ of semiconducting SWCNTs at 100 MHz, and increases Λ about two times at 10 MHz. Thus the coating strongly increases Λ for metallic SWCNTs and slightly increases Λ for semiconducting SWCNTs. This was also noted in[27] for coated nanospheres.

It should be noted that according to Figs. 8 and 9 the coating practically does not change the values of Λ and θ for SWCNTs at high host conductivity ($\sigma_w>0.1$ S m^{-1}) and frequency 100 MHz. That means the presence of a coating will be ineffective at high megahertz frequencies and high host conductivities.

Figure 10 shows the dependence of the normalized absorption cross section Λ of coated metallic SWCNTs on the host conductivity at different relative dielectric constants of the coating. The value of Λ increases with increasing the magnitude $\mathrm{Im}[\varepsilon_s]$ and decreasing the value $\mathrm{Re}[\varepsilon_s]$.

IV. CONCLUSIONS

In conclusion, the model of finite-length SWCNTs coated with a dielectric is developed. In practice, for aqueous environments the dielectric models a layer of surfactant. The absorption cross section of SWCNTs, MWCNTs, and bundles of SWCNTs in a conductive host are calculated in the radio frequency range. The mechanism of energy dissipation enhancement in the conductive host due to strong local field enhancement near the SWCNT is established. It has been shown that for energy dissipation enhancement SWCNTs are preferable to MWCNTs and SWCNT-bundles at the same mass fraction of CNT inclusions. It has been demonstrated that the presence of a lossy coating can increase the absorption cross-section of carbon nanotubes in

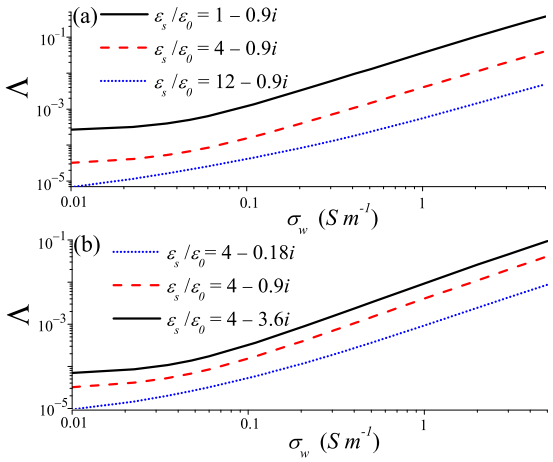

FIG. 10. (Color online) Normalized absorption cross section Λ of coated (15,0) metallic SWCNTs vs the host conductivity σ_w at different real (a) and imaginary (b) parts of coating relative dielectric constant $\varepsilon_s\varepsilon_0/$. The frequency is 10 MHz, $L=0.8$ μm, and the external radius of the coating is 3.4 nm.

Downloaded 01 Dec 2010 to 129.89.58.128. Redistribution subject to AIP license or copyright; see http://jap.aip.org/about/rights_and_permissions

the rf range. Thus, the analysis carried out in this paper forms the basis for development and optimization of experiments for therapeutic applications, including selective thermolysis of cancer cells and thermoacoustic imaging.

ACKNOWLEDGMENTS

This research was partially supported by the Belarus Republican Foundation for Fundamental Research (BRFFR) under Project Nos. F10R-002 and F10CO-020, EU FP7 under Project Nos. FP7-230778 TERACAN and FP7-266529 BY-NanoERA, and ISTC Project No. B-1708.

APPENDIX: APPROXIMATE EXPRESSIONS FOR THE ELECTRIC FIELD INSIDE THE DIELECTRIC COATING OF SWCNTS

The aim of the Appendix is the derivation of an approximate analytical expression for the electric field inside the dielectric coating. Our approach is based on the assumption that the scattered field near the SWCNT surface at a point with coordinate z is induced mainly by the current in the interval $[z-h,z+h]$, where $R \ll h < L/20$.

Let us proceed from the expression for electric field scattered by a SWCNT determined according to Eq. (9) as

$$E_z^{(c)}(\rho,z) = \frac{R}{i\omega\varepsilon_w}\int_{-L/2}^{L/2} j^{(c)}(z') \times \int_0^{2\pi}\left(\frac{\partial^2}{\partial z^2}+k^2\right) g(z-z',\rho,R,\phi)\,d\phi\,dz', \tag{A1}$$

$$E_\rho^{(c)} = \frac{R}{i\omega\varepsilon_w}\int_{-L/2}^{L/2} j^{(c)}(z')\int_0^{2\pi}\frac{\partial^2}{\partial z\,\partial\rho} g(z-z',\rho,R,\phi)\,d\phi\,dz'. \tag{A2}$$

After replacement $\partial g(z-z',\rho,R,\phi)/\partial z \to -\partial g(z-z',\rho,R,\phi)/\partial z'$ in Eq. (A2) and integration by parts with application of the edge condition for SWCNT current $j^{(c)}(\pm L/2)=0$ we arrive to the expression for $E_\rho^{(c)}(z,\rho)$,

$$E_\rho^{(c)} = \frac{R}{i\omega\varepsilon_w}\frac{\partial}{\partial\rho}\int_0^{2\pi}\int_{-L/2}^{L/2}\frac{\partial j^{(c)}(z')}{\partial z'} g(z-z',\rho,R,\phi)\,dz'\,d\phi. \tag{A3}$$

As the function $g(z-z',\rho,R,\phi)$ quickly decreases with increasing the value $z-z'$ the main contribution of the integration over z' comes from the small vicinity near point z. This permits one to suppose $\partial j^{(c)}(z')/\partial z' \cong \partial j^{(c)}(z)/\partial z$ for points located far from the edges $|z| \le L/2-5R$ and change the integration limits

$$\int_{-L/2}^{L/2}\{\ldots\}dz' \to \int_{-\infty}^{\infty}\{\ldots\}dz'. \tag{A4}$$

Then, Eq. (A3) can be transformed as

$$E_\rho^{(c)} \cong \frac{R}{i\omega\varepsilon_w}\frac{\partial j^{(c)}(z)}{\partial z}\frac{\partial}{\partial\rho}\int_0^{2\pi}\int_{-\infty}^{\infty} g(z-z',\rho,R,\phi)\,dz'\,d\phi. \tag{A5}$$

From Eq. (A5) we can calculate $E_\rho^{(c)}$ in the quasistatic limit $(k\to 0)$ as

$$E_\rho^{(c)}(z,\rho) \cong -\frac{R}{i\omega\varepsilon_w\rho}\frac{\partial j^{(c)}}{\partial z} \quad \text{if} \quad \begin{cases} R<\rho<b \\ |z|<L/2 \end{cases}. \tag{A6}$$

Numerical calculation shows that Eq. (A6) is a good approximation of Eq. (A2) for all points near the SWCNT surface, with the exception of the CNT edges. The range of inapplicability of Eq. (A6) is very narrow, $|z| > L/2-5R$, and their contribution into the SWCNT response is small and can be neglected. Therefore, we shall apply approximate Eq. (A6) along the entire tube.

Let us now calculate the scattered field $\mathbf{E}^{(d)}$. From Eq. (10) in the quasistatic limit $(k\to 0)$ we have

$$\begin{aligned}\mathbf{E}^{(d)} &\cong \frac{1}{i\omega\varepsilon_w}\mathrm{grad}\ \mathrm{div}\int_V \mathbf{e}_{\rho'} j_{\rho'}(\mathbf{r}')\, g_0(|\mathbf{r}-\mathbf{r}'|)\,d\mathbf{r}' \\ &= \frac{-1}{i\omega\varepsilon_w}\mathrm{grad}\int_V \mathrm{div}_{\mathbf{r}'}\{\mathbf{e}_{\rho'} j_{\rho'}(\mathbf{r}')\, g_0(|\mathbf{r}-\mathbf{r}'|)\}\,d\mathbf{r}' \\ &\quad + \frac{1}{i\omega\varepsilon_w}\mathrm{grad}\int_V g_0(|\mathbf{r}-\mathbf{r}'|)\mathrm{div}_{\mathbf{r}'}\{\mathbf{e}_{\rho'} j_{\rho'}(\mathbf{r}')\}\,d\mathbf{r}',\end{aligned} \tag{A7}$$

where $g_0 = 1/4\pi(|\mathbf{r}-\mathbf{r}'|)$ is the Green function in the quasistatic limit. The first term on the right of Eq. (A7) equals zero. Then, the radial and axial components of the vector $\mathbf{E}^{(d)}$ are

$$E_\rho^{(d)}(z,\rho) = \frac{1}{i\omega\varepsilon_w}\int_0^b\int_0^{2\pi}\int_{-L/2}^{L/2}\frac{\partial}{\partial\rho} g_0(z-z',\rho,\rho',\phi) \times \frac{\partial(\rho' j_{\rho'})}{\partial\rho'}dz'\,d\phi\,d\rho', \tag{A8}$$

$$E_z^{(d)}(z,\rho) = \frac{1}{i\omega\varepsilon_w}\int_0^b\int_0^{2\pi}\int_{-L/2}^{L/2}\frac{\partial}{\partial z} g_0(z-z',\rho,\rho',\phi) \times \frac{\partial(\rho' j_{\rho'})}{\partial\rho'}dz'\,d\phi\,d\rho'. \tag{A9}$$

For points inside the dielectric coating analogous to Eq. (A2) in Eqs. (A8) and (A9) we shall suppose $j_\rho(z')=j_\rho(z)$ and make replacement (A4). Then, Eq. (A8) can be reduced to the following expression

$$E_\rho^{(d)}(z,\rho) = \frac{1}{i\omega\varepsilon_w}\int_0^b\frac{\partial(\rho' j_{\rho'})}{\partial\rho'} \times\frac{\partial}{\partial\rho}\int_0^{2\pi}\int_{-\infty}^{\infty} g(z-z',\rho,\rho',\phi)dz'\,d\phi\,d\rho'. \tag{A10}$$

After integration over z' and ϕ in Eq. (A10) analogically to Eq. (A5) and simple integration over ρ' we have

Downloaded 01 Dec 2010 to 129.89.58.128. Redistribution subject to AIP license or copyright; see http://jap.aip.org/about/rights_and_permissions

$$E_{\rho}^{(d)} \cong -\frac{j_{\rho}}{i\omega\varepsilon_w}, \quad \begin{cases} R < \rho < b \\ |z| < L/2 \end{cases}. \tag{A11}$$

After substitution of Eqs. (A6) and (A11) into Eq. (4) we have

$$j_{\rho} = \sigma(E_{\rho}^{(d)} + E_{\rho}^{(c)}) = \frac{\varepsilon_w \sigma}{\varepsilon_s} E_{\rho}^{(c)} = -\frac{R\sigma}{i\omega\varepsilon_s \rho}\frac{\partial j^{(c)}}{\partial z}. \tag{A12}$$

Equation (A9) after the differentiation over z and the replacements (A4) and $j_{\rho'}(z') \to j_{\rho'}(z)$ has the form

$$E_z^{(d)} \cong \frac{1}{4i\pi\omega\varepsilon_w}\int_0^b \frac{\partial(\rho' j_{\rho'})}{\partial\rho'}\int_0^{2\pi}\int_{-\infty}^{\infty}\frac{(z-z')}{|\mathbf{r}-\mathbf{r}'|^3}d\rho' d\phi dz'. \tag{A13}$$

The subintegral function in Eq. (A13) is odd with respect to $z'-z$ and give zero contribution to Eq. (A13) after integration over z'. Thus, we can conclude that $E_z^{(d)}|_{\rho\in[R,b]} \ll E_z^{(c)}|_{\rho\in[R,b]}$. It is not difficult to show that the inequality $E_z^{(d)} \ll E_z^{(c)}$ is true for any point on the space. So, the z component of the total field is determined mainly as a superposition of the incident field and the z-component of the electric field scattered by the SWCNT,

$$E_z \cong E_0 + E_z^{(c)}. \tag{A14}$$

Approximate expressions (A5), (A6), and (A11) are the result of the Appendix. They hold true near the SWCNT surface at $|z| \le L/2-5R$ (not close to the SWCNT edges) in the approximation of negligibly small axial depolarizing field of SWCNT coating.

[1] S. Reich, C. Thomsen, and J. Maultzsch, *Carbon Nanotubes: Basic Concepts and Physical Properties* (Wiley, New York, 2004).
[2] G. Y. Slepyan, S. A. Maksimenko, A. Lakhtakia, O. Yevtushenko, and A. V. Gusakov, Phys. Rev. B **60**, 17136 (1999).
[3] S. A. Maksimenko and G. Y. Slepyan, in *Electromagnetic Fields in Unconventional Materials and Structures*, edited by O. N. Singh and A. Lakhtakia (Wiley, New York, 2000), pp. 217–255.
[4] J. Hagmann, IEEE Trans. Nanotechnol. **4**, 289 (2005).
[5] G. Miano and F. Villone, IEEE Trans. Antennas Propag. **54**, 2713 (2006).
[6] S. Salahuddin, M. Lundstrom, and S. Datta, IEEE Trans. Electron Devices **52**, 1734 (2005).
[7] Y. Wang, K. Kempa, B. Kimball, G. Benham, W. Z. Li, T. Kempa, J. Rybczynski, A. Herczynski, and Z. F. Ren, Appl. Phys. Lett. **85**, 2607 (2004).
[8] G. W. Hanson, IEEE Trans. Antennas Propag. **53**, 3426 (2005).
[9] G. Y. Slepyan, M. V. Shuba, S. A. Maksimenko, and A. Lakhtakia, Phys. Rev. B **73**, 195416 (2006).
[10] P. J. Burke, S. Li, and Z. Yu, IEEE Trans. Nanotechnol. **5**, 314 (2006).
[11] J. Chen, V. Perebeinos, M. Freitag, J. Tsang, Q. Fu, J. Liu, and P. Avouris, Science **310**, 1171 (2005).
[12] M. E. Portnoi, O. V. Kibis, and M. Rosenau da Costa, Superlattices Microstruct. **43**, 399 (2008).
[13] K. G. Batrakov, S. A. Maksimenko, P. P. Kuzhir, and C. Thomsen, Phys. Rev. B **79**, 125408 (2009).
[14] N. W. S. Kam, M. O'Connell, J. A. Wisdom, and H. Dai, Proc. Natl. Acad. Sci. U.S.A. **102**, 11600 (2005).
[15] B. Panchapakesan, S. Lu, K. Sivakumar, K. Teker, G. Cesarone, and E. Wickstrom, NanoBiotechnology **1**, 133 (2005).
[16] J.-W. Kim, E. V. Shashkov, E. I. Galanzha, N. Kotagiri, and V. P. Zharov, Lasers Surg. Med. **39**, 622 (2007).
[17] S. V. Torti, F. Byrne, O. Whelan, N. Levi, B. Ucer, M. Schmid, F. M. Torti, S. Akman, J. Liu, P. M. Ajayan, O. Nalamasu, and D. L. Carroll, Int. J. Nanomed. **2**, 707 (2007).
[18] C.-H. Wang, Y.-J. Huang, and C.-A. Peng, Proceedings of ICBME, edited by C. T. Lim and J. C. H. Goh, 2009, Vol. 23, p. 888.
[19] H. K. Moon, S. H. Lee, and H. C. Choi, ACS Nano **3**, 3707 (2009).
[20] C.-H. Wang, Y.-J. Huang, C.-W. Chang, W.-M. Hsu, and C.-A. Peng, Nanotechnology **20**, 315101 (2009).
[21] A. Burkea, X. Dingb, R. Singha, R. A. Kraftb, N. L. Polyachenkoc, M. N. Rylanderd, C. Szotd, C. Buchanand, J. Whitneyd, J. Fisherd, H. C. Hatchera, R. D'Agostino, Jr., N. D. Kockg, P. M. Ajayanh, D. L. Carrollf, S. Akmana, F. M. Tortia, and S. V. Tortif, Proc. Natl. Acad. Sci. U.S.A. **106**, 12897 (2009).
[22] F. Zhou, D. Xing, Z. Ou, B. Wu, D. E. Resasco, and W. R. Chen, J. Biomed. Opt. **14**, 021009 (2009).
[23] A. Burlaka, S. Lukin, S. Prylutska, O. Remeniak, Yu. Prylutskyy, M. Shuba, S. Maksimenko, U. Ritter, and P. Scharff, J. Exp. Ther. Oncol. **32**, 48 (2010).
[24] M. Pramanik, M. Swierczewska, D. Green, B. Sitharaman, and L. V. Wang, J. Biomed. Opt. **14**, 034018 (2009).
[25] A. de la Zerda, C. Zavaleta, S. Keren, S. Vaithilingam, S. Bodapati, Z. Liu, J. Levi, B. R. Smith, T. J. Ma, O. Oralkan, Z. Cheng, X. Chen, H. Dai, B. T. Khuri-Yakub, and S. S. Gambhi, Nat. Nanotechnol. **3**, 557 (2008).
[26] D. O. Lapotko, Nanomedicine **4**, 813 (2009).
[27] G. W. Hanson and S. K. Patch, J. Appl. Phys. **106**, 054309 (2009).
[28] A. Mashal, B. Sitharaman, X. Li, P. K. Avti, A. V. Sahakian, J. H. Booske, and S. C. Hagness, IEEE Trans. Biomed. Eng. **57**, 1831 (2010).
[29] C. J. Gannon, P. Cherukuri, B. I. Yakobson, L. Cognet, J. S. Kanzius, C. Kittrell, R. B. Weisman, M. Pasquali, H. K. Schmidt, R. E. Smalley, and S. A. Curley, Cancer **110**, 2654 (2007).
[30] Y. Chen, I. J. Craddock, and P. Kosmas, IEEE Trans. Biomed. Eng. **57**, 1003 (2010).
[31] J. D. Shea, P. Kosmas, B. D. V. Veen, and S. C. Hagness, Inverse Probl. **26**, 074009 (2010).
[32] V. Raicu, T. Saibara, H. Enzan, and A. Irimajiri, Bioelectrochem. Bioenerg. **47**, 333 (1998).
[33] M. V. Shuba, S. A. Maksimenko, and G. Y. Slepyan, J. Comput. Theor. Nanosci. **6**, 2016 (2009).
[34] L. A. Weinstein, *The Theory of Diffraction and the Factorization Method* (Golem, New York, 1969).
[35] M. V. Shuba, S. A. Maksimenko, and A. Lakhtakia, Phys. Rev. B **76**, 155407 (2007).
[36] M. V. Shuba, G. Ya. Slepyan, S. A. Maksimenko, C. Thomsen, and A. Lakhtakia, Phys. Rev. B **79**, 155403 (2009).
[37] G. Y. Slepyan, M. V. Shuba, S. A. Maksimenko, C. Thomsen, and A. Lakhtakia, Phys. Rev. B **81**, 205423 (2010).
[38] C. Beard, J. L. Blackburn, and M. J. Heben, Nano Lett. **8**, 4238 (2008).
[39] X. Zhou, J.-Y. Park, S. Huang, J. Liu, and P. L. McEuen, Phys. Rev. Lett. **95**, 146805 (2005).
[40] S. V. Prylutska, I. I. Grynyuk, O. P. Matyshevska, V. M. Yashchuk, Y. I. Prylutskyy, U. Ritter, and P. Scharff, Physica E **40**, 2565 (2008).

Downloaded 01 Dec 2010 to 129.89.58.128. Redistribution subject to AIP license or copyright; see http://jap.aip.org/about/rights_and_permissions